Accepted Manuscript

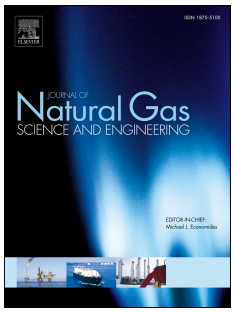

Simulating Yield Stress Variation along Hydraulic Fracture Face Enhances Polymer Cleanup Modeling in Tight Gas Reservoirs

Regina Tayong A, Mustafa M. Alhubail, Belladonna Maulianda, Reza Barati

PII: S1875-5100(19)30044-7

DOI: https://doi.org/10.1016/j.jngse.2019.02.006

Reference: JNGSE 2829

To appear in: *Journal of Natural Gas Science and Engineering*

Received Date: 21 September 2018

Revised Date: 15 February 2019

Accepted Date: 18 February 2019

Please cite this article as: Tayong A, R., Alhubail, M.M., Maulianda, B., Barati, R., Simulating Yield Stress Variation along Hydraulic Fracture Face Enhances Polymer Cleanup Modeling in Tight Gas Reservoirs, *Journal of Natural Gas Science & Engineering*, https://doi.org/10.1016/j.jngse.2019.02.006.

Simulating Yield Stress Variation along Hydraulic Fracture Face Enhances Polymer Cleanup Modeling in Tight Gas Reservoirs

Regina Tayong A., Mustafa M. Alhubail [a], Belladonna Maulianda[b], Reza Barati [a,*]

[a] Chemical and Petroleum Engineering Department, The University of Kansas, Learned Hall, 1530 W. 15th St., Lawrence KS 66045, USA

[b] Petroleum Engineering Department, Universiti Teknologi PETRONAS, Seri Iskandar 32610, Perak, Malaysia

*Corresponding author
Email address: rezab@ku.edu (Reza Barati) [*]

Abstract

Several measures have been taken to enhance the supply of fossil fuel energy in the United States during the last decades, some of which include the development and exploitation of very low permeability and low porosity reservoirs in challenging environments. These reservoirs usually require enhanced stimulation techniques such as multi-stage hydraulic fracturing and horizontal drilling to increase the contact between the wellbore and the producing formation for a profitable recovery. During the fracturing process, fluids are pumped into the reservoir under high pressure, to create fractures through which gas flows back to the earth's surface during production. However, a layer of concentrated polymer forms on the fracture faces limiting the loss of fluid to the formation during injection while impairing fracture conductivity during production. The inadequacy of the fracture conductivity after a fracture treatment using cross-linked fluids is typically due to poor degradability of our polymers, proppant crushing, clay swelling in the case of incompatible fluids and formation damage. The objective of this work is to develop a fracture cleanup model that simulates the rheological variations of filter cake and degraded fluids inside the fracture by including the effect of breaker and polymer concentration on the yield stress of the fracturing fluid that result in variations in capillary pressure, fracture conductivity, fracture length and formation damage during the cleanup process in unconventional tight gas formations.

A dynamic 2-D, three-phase IMPES simulator, incorporating a yield-power-law-rheology (Herschel-Buckley fluids), has been developed in MATLAB to simulate variations in rheological properties of degrading fracturing fluids versus time and investigate the influence of several major parameters on the fracture cleanup process. These parameters include variations in polymer concentration along the fracture length, breaker concentration variations, fracture conductivity, fracture length, capillary pressure and formation damage with a novel correlation between yield stress and breaker concentration, which enhances post – fracture well performance prediction in tight gas reservoirs. The three phases simulated here include water, gas and the gel phases.

Simulation of the injection of fracturing fluids and fluid imbibition during the shut-in time indicated that for tight gas formations, fluid recovery increases with increasing shut-in time, increasing fracture conductivity and fracture length irrespective of the yield stress of the fracturing fluid. Simulation of the production phase highlighted that increasing the capillary

pressure to a maximum of 350.10 psi resulted in a 10.4% decrease in cumulative gas production. The rate of increase in the yield stress of the fracturing fluid along the fracture face is proportional to the square of the volume of fluid loss to the formation. Production will be enhanced significantly with increasing breaker concentration indicating that simulation of the yield stress variation along the fracture face presents a more realistic scenario of the fracture cleanup process rather than assuming a constant value since the fluid loss to the formation and the polymer concentration distribution decrease with fracture length.

Keywords: Hydraulic Fracture, Cleanup Model, Yield Stress, Formation Damage, Unconventional Reservoirs, Guar Based Fluids

1 Introduction

Hydraulic fracturing has been successfully applied in horizontal, directional and vertical wells, and in both conventional and unconventional formations, increasing productivity through increased contact between wellbore and producing reservoir (Zoveidavianpoor & Gharibi, 2015). During the fracturing process, fluids (typically a mixture of water, proppant and chemical additives) are pumped at sufficiently high pressures to crack the rock open, and propagate the fracture through the formation under very high injection rates. Some of the fracturing fluid leaks off into the formation to create the invaded zone, leaving back polymer residues that form the filter cake on both faces of the fracture (Odumabo, Karpyn, & Ayala, 2014). **Figure 1** shows the invasion zone simulated in this study due to the continuous loss of fluids into the formation. Filter cake occupies the entire pore space of the propped fracture following the fracture closure (Ayoub, et al., 2006). Fracturing fluids should be viscous enough to carry the proppant along the fracture and be easily degraded after injection to sustain a highly conductive path in the fracture during production. Guar based fluids are frequently used as fracturing fluids during injection. Cross-linkers such as borates and zirconates and delayed breakers, either oxidizers or enzymes, are added to the fluid to degrade the polymer gel and filter cake formed before the start of production (Economides & Nolte, 2000). Polymer concentration varies along the fracture length due to different exposure times to fracturing fluid and different proppant concentrations along the fracture (Seright, 2004).

At the end of the fracturing treatment process, the well is shut-in to allow for fracture closure during which fluid filtrate continues to leak off into the matrix, thereby increasing the concentration of polymer formed on the fracture face. The thickness of the filter cake formed is a function of the type of the fracturing fluid that is used, reservoir properties, pressure gradients between reservoir and fracture and the erosional effect of the slurry on the fracture face (Davies & Kuiper, 1988).

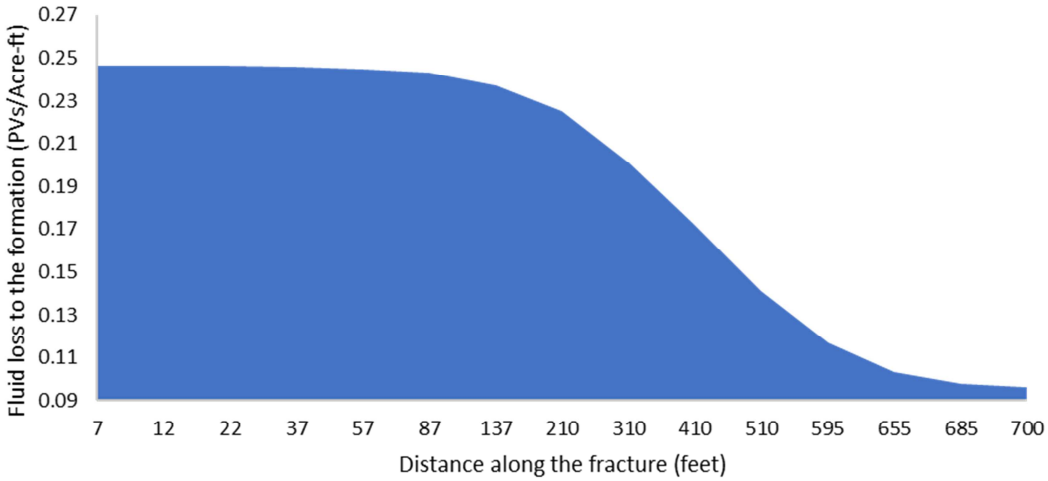

Figure 1: Schematic picture of the invasion zone created in the reservoir after fracture treatment

The gas flow mechanism in the reservoir will change from radial to linear flow after a successful fracture treatment (Holditch & Tschirhart, 2005). Concentrated polymer residue on the fracture face generates a yield stress, which requires a minimum pressure gradient to begin the cleanup process in the proppant pack (May, Britt, & Nolte, 1997). During the cleanup process, fluids flow through the fracture back out of the well, leaving behind the proppant that help to keep the newly created fissures open. These fissures typically extend into the formation enabling oil and gas to flow from pores within the formation to the producing well. The initial fluid that returns to the surface is usually termed "flow back" and the fluid that flows from the well along with oil and gas during the production phase is often referred to as "produced fluid''. Long cleanup periods following a fracture treatment are typically due to a combination of poorly degraded polymer fluids, low formation pressures and/-or large retained liquid volumes. The joint effects of non-Darcy flow, stress dependency of reservoir permeability, fracture closure and high capillary pressure in the matrix can reportedly contribute to a 40% cut in production over a 10-year period under realistic conditions (Friedel, 2006).

The severity of formation damage varies with reservoir characteristics and is most commonly dependent on the kind of wellbore fluids used. It may occur near the wellbore region of a well or extend deep into the formation, resulting in a reduction in permeability and adversely curtailing productivity. Mechanical, chemical and hydraulic damage to the reservoir have resulted from hydraulic fracturing process. Mechanical damage typically results from broken polymer/fines migration into the reservoir matrix under very high fluid shear rates, external solids entrainment that plug formation pores, phase trapping and blocking, perforation damage, proppant crushing and embedment. Chemical damage is caused by adverse rock-fluid interactions, adverse fluid-fluid interactions and near wellbore wettability alterations resulting in clay swelling, clay de-flocculation, formation dissolution, pore plugging and a switch from water-wet to oil-wet conditions (Færgestad, 2016). Hydraulic damage in the invaded zone arises from the increase in water saturation during leak-off, which causes a shift in capillary pressures to higher values, a reduction in gas relative permeability and relative permeability hysteresis in the invaded zone. However, mechanically induced formation damage combined with hydraulic damage tends to be the most significant for low permeability reservoirs as it results in switching

to higher capillary pressure curves and lower effective permeability for the hydrocarbon phase (Qutob & Byrne, 2015).

This study has been designed to create a better understanding of the fracture treatment process and the shortcomings of its application in tight gas reservoirs by considering the rheology of filter cake and degraded fluids inside the fracture and examining the influence of breaker concentration, polymer concentration, varying yield stress of filter cake, capillary pressure, fracture conductivity, fracture length and formation damage on the cleanup process in unconventional tight gas formations using a 2-D three phase model.

2 Literature Review

Several simulators have been reported in the literature for investigating fracture face damage mechanisms and factors affecting fracturing fluid cleanup in hydraulically fractured wells. A critique of relevant work done in this area is summarized in the following three subsections.

2.1 Simulations of Holditch and Wang et al.

Holditch (Holditch, 1979) used a single-phase 2-D finite difference model to simulate the effects of reservoir permeability damage around a fracture and a fully implicit two phase, two-dimensional model to investigate the effects of relative permeability and capillary pressure on the productivity of fractured reservoirs.

Holditch identified three distinct permeability zones: the reservoir, fracture and the damaged zone. Capillary pressure calculated for each region was by means of the measured Leverett J-function for the desired rock type, as given in Eq. 1**,**

$$P_c = \sigma \cos(\theta) J(S_w) \sqrt{\frac{\varphi}{k}} \qquad \textit{Eq. 1}$$

where P_c is the capillary pressure in (kPa), σ is the interfacial tension in (mN/m), the permeability k is in md and J, the Leverett *J*-function

Holditch concluded that the effect of formation damage was significant only if it was several inches deep and reduced the formation permeability by a factor of 100 or more. Secondly, the relative permeability damage alone will restrict gas production only when the injected fluid is not easily removed from the invaded zone. Finally, his results indicated that the damaged zone permeability must be reduced by several orders of magnitude and the capillary pressure altered before a serious water block to gas flow will occur.

Wang et al. (Wang, Holditch, & McVay, 2010) (Wang, Holditch, & McVay, 2012) used a three dimensional three-phase black oil simulator to simulate the effects of gel residue, filter cake formation and yield stress on fracturing fluid clean up and long term gas recovery in tight gas formation. They validated their model against Voneiff's et al. work (Voneiff, Robinson, & Holditch, 1996) for Newtonian fluid flow without yield stress and Friedel's model (Friedel, 2006) for Herschel Buckley fluids with finite yield stress values. Wang et al. concluded that if the fracturing fluid breaks down to a Newtonian fluid, then a dimensionless fracture conductivity of 10 or greater is suitable for optimizing gas production and fracturing fluid cleanup. If the

fracturing fluid does not break but retains a gel strength of 3-100 Pa, then the fracturing fluid either cleans up slowly or never cleans up when a dimensionless fracture conductivity value of 10 or less is applied.

2.2 Simulations of Gdanski et al.

In 2005, Gdanski et al. (Gdanski, Weaver, Slabaugh, Walters, & Parker, 2005) modeled the effect of formation damage in the invaded zone by correlating the capillary function with the Leverett J-function. The resulting equation was used in modeling of capillary pressure in the matrix.

$$P_c = \frac{\sigma}{a_2 S_w^{a1}} \left(\frac{\varphi}{k}\right)^{a3} \qquad Eq.\ 2$$

where P_c is the capillary pressure, $\boldsymbol{\sigma}$ is the surface tension and a1, a2 and a3 are adjustable constants.

Now considering Eq. 2, mechanical damage resulting in lower matrix permeability raises the capillary pressure in the damaged zone causing an influx of water from the undamaged matrix. Higher water saturation in the damaged zone adversely affects gas production. After varying the relative permeability to gas for constant water curve, Gdanski et al. observed that water production was equally a function of gas relative permeability in which lowering the gas permeability at high water saturations raised the pressure near the fracture face and consequently water production. Gdanski et al. postulated that the relative permeability and capillary pressure changes were unimportant for the undamaged matrix if high capillary pressure imbibed more water into the reservoir and a high-pressure drawdown existed to overcome the capillary pressure differences between the invaded and the unadulterated portions of the formation. They calculated the skin factor on the face of the fracture from Eq. 3**,**

$$s = \left(\frac{k}{k'} - 1\right)\left(\frac{\pi w}{2x_f}\right) \qquad Eq.\ 3$$

where x_f and w are the fracture half-length and the depth of fracture-face damage, respectively, and k and k' are the permeability of undamaged and damaged zones, respectively.

In 2006, using the same model Gdanski et al. (Gdanski, Fulton, & Shen, 2006), made improvements on previously published results after considering that the apparent lower fracture face skin could be due to pressure drop across the damaged zone that lowers gas density and viscosity. Skin factor calculations for m number of cells along the fracture and n-1 number of invaded cells perpendicular to the fracture were modified to

$$s = \left(\frac{\pi}{2x_f}\right) \sum_{j=2}^{n} wj \left(\frac{\left(\frac{k_g}{\mu_g}\right)_0 x_f}{\sum_{i=1}^{m} \left(\frac{k_g}{\mu_g}\right)_{i,j} L_I} - 1\right) \qquad Eq.\ 4$$

where $\left(\frac{k_g}{\mu_g}\right)_0$ the undamaged mobility to gas is measured at the reference point (0), L_i and W_j are length of i cells and width of j cells, respectively.

Finally, in 2009, Gdanski et al. (Gdanski, Fulton, & Shen, 2009) used a new backward difference scheme on a two-phase, two-dimensional model to demonstrate that the fracture face skin relative to gas flow can be calculated continually throughout a fracturing treatment cleanup and production process using an expansion of the classical Cinco-Ley and Samaniego fracture face skin equation. Gdanski et al. established that the effect of water saturation in the damaged zone becomes much more significant for lower permeability and higher capillary pressures in the matrix and that the effective fracture face skin relative to gas could be several times higher than expected from a single-phase flow. Conclusively, their results demonstrated that there would always be a higher fracture face skin to gas in the smectite-swelling scenario than in the kaolinite dispersion scenario. In addition, for tight gas reservoirs (~0.01 md or less), even a small amount of matrix damage could result in high fracture face skins and significantly prolong cleanup times. In addition, tight gas reservoirs were reportedly much more susceptible to water blocking by clay damage than formations with higher permeability.

2.3 Simulations of Friedel and Barati et al.

Friedel (Friedel, 2006) developed a fast and stable fully implicit, three-phase black oil simulator capable of modeling YPL behavior of fracturing fluids flowing through the proppant pack. The equations of power law behavior after gel yielding and yield stress were obtained from the work of Al-Fariss et al. (Al-Fariss & Pinder, 1984). The algorithm for choosing suitable grids for fractured wells was determined by Bennett et al. (Bennett, Reynolds, Raghavan, & Elbel, 1986). It is designed to create finer grids near the fracture face, wellbore and fracture tip. Only a quarter of the drainage area from the fracture was simulated, as there are two wings for the fractures and two faces for each fracture, assuming a symmetric fracture that extends equal distances on both sides of the wellbore and fully penetrates the formation. Friedel investigated the effects of non-Darcy flow and stress dependency of tight reservoir rocks, usually neglected in most fracturing fluid cleanup studies. He concluded that inertial effects were more influential than other effects in the fracture, but non-Darcy effects if neglected will result in an overestimation of production. Furthermore, he stated that the combined effects of permeability dependence on stress and non-Darcy effects decreased production by 40% compared to the case without non-Darcy flow. These observations were supported by other researchers in the field (Al-Rbeawi, 2016; Al-Rbeawi, 2018).

In 2009, Barati et al. (Barati, et al., 2009) modified Friedel's model (Friedel, 2006) and further investigated the fracturing cleanup process in tight gas formations with permeability of 0.005 md and greater. This model was validated against type curves published by Argarwal et al. (Agarwal, Carter, & Pollock, 1979) for a single well connected with a finite conductivity fracture in an infinite reservoir producing under constant pressure, to ratify that the fine-grid system around the fracture did not affect the material balance calculations. After a thorough analysis of the effects of capillary pressure, yield stress, conductivity and mechanical damage on the fracturing fluid cleanup process, Barati et al. concluded that the model with Bennett gridding accurately represented the transient response of a hydraulically fractured well. Capillary pressure caused the leak off water to be imbibed deeper into the reservoir. Increasing the capillary pressure had insignificant effects on gas and gel production but not on water production. Also, gel production increases with increasing fracture conductivity only if the pressure gradient along the fracture is greater than the yield stress needed for the fluid to move for low permeability formations. However, if the permeability is increased above 5 md, yield stress effects become insignificant. Finally, Barati et al. stated that the effects under consideration become less

significant when the reservoir permeability exceeds 5 md for the conditions modelled and all the studied effects became severely more significant for tight and ultra-tight cases in their study.

3 Simulation Methodology

Simulation studies for this project were conducted in two parts. To begin with, a three-phase simulator was developed in MATLAB using a 2-D structured grid system. This model is very fast and stable and has the capabilities of handling both anisotropic/isotropic, homogeneous/heterogeneous as well as different types of boundary conditions. This simulator was validated by solving the three-phase flow exercise provided in the Basic Applied Reservoir simulation textbook (Ertekin, Abou-kassem, & King, 2001). Fluid PVT Data, relative permeability and capillary pressure curves imported into the Simulator were gotten from the A-1 reservoir situated in Plum Bush Creek field, Washington County, Colorado. History matching for all the five wells reported for this field was very successful, which adequately validates our 2-D three phase model.

3.1 Model Validation

The developed three-phase simulator was validated against a standard case study that is reported in the Basic Applied Reservoir Simulation textbook for both operating conditions (i.e., pressure specified and rate specified cases) (Ertekin, Abou-kassem, & King, 2001). The validation for the pressure specified case is shown in **Figure 2-Figure 5**, and the validation for the rate specified case is shown in **Figure 6-Figure 9**.

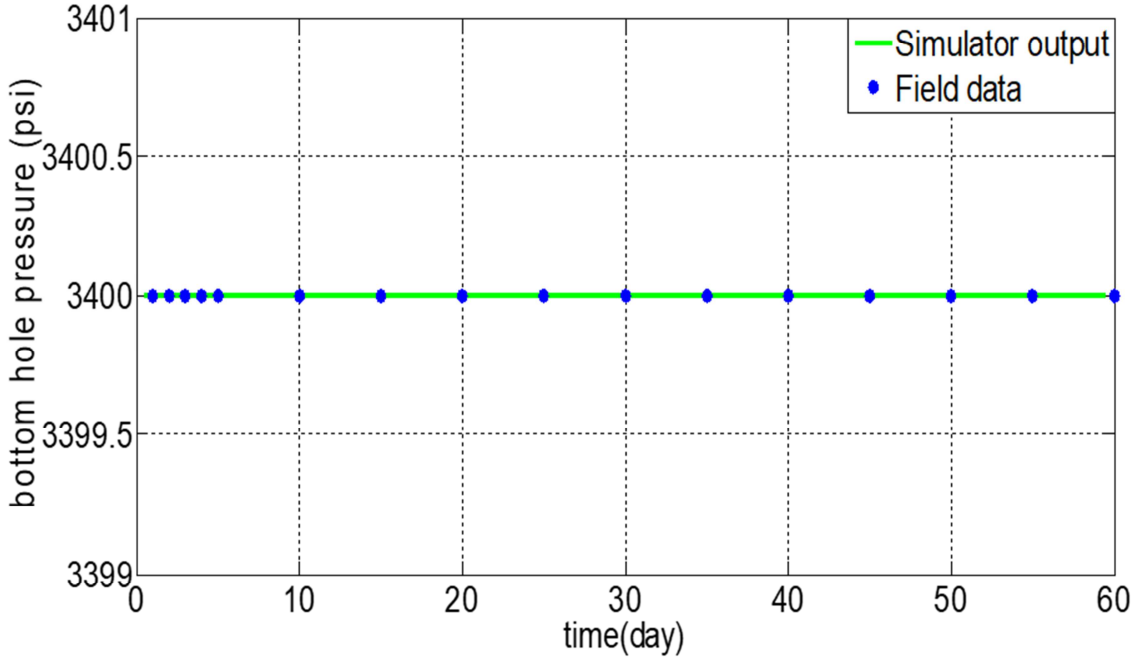

Figure 2: Bottom-hole pressure for pressure specified well, (W-2)

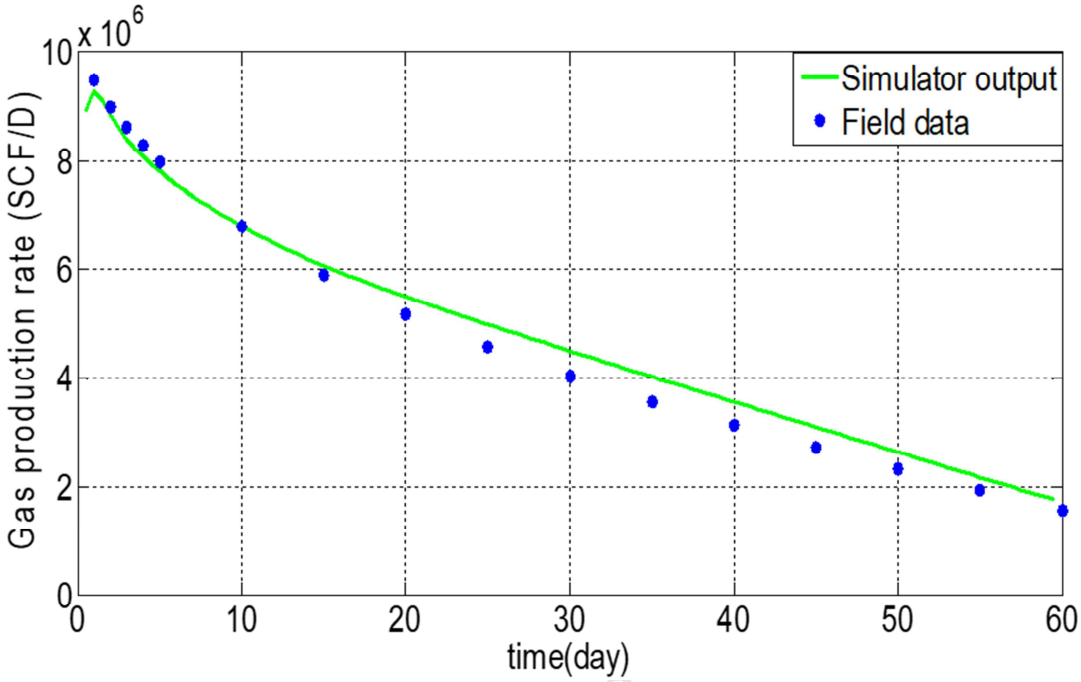

Figure 3: Gas production rate for pressure specified well, (W-2)

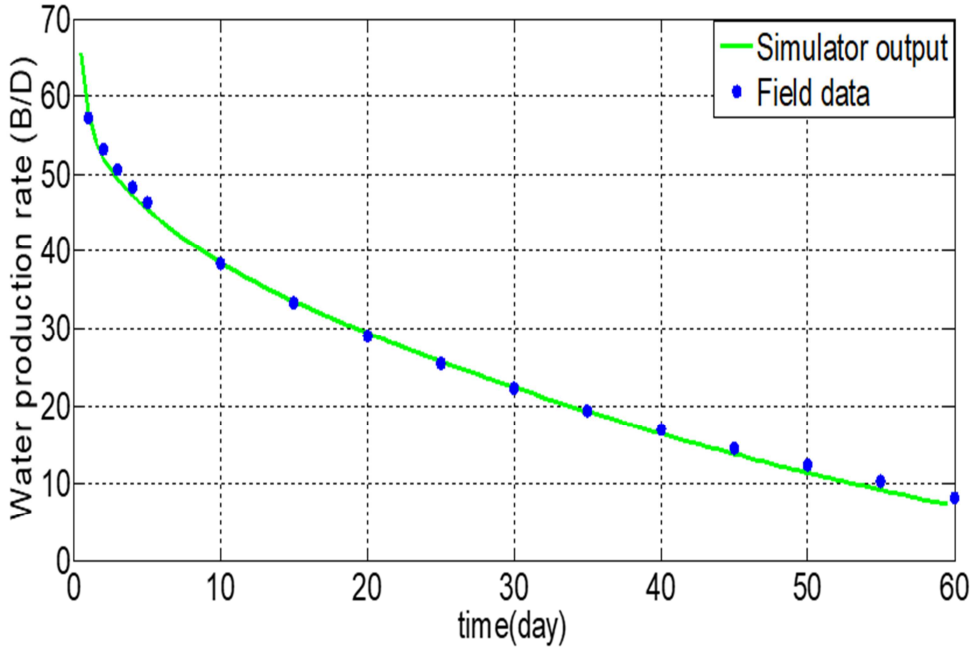

Figure 4: Water production rate for pressure specified well, (W-2)

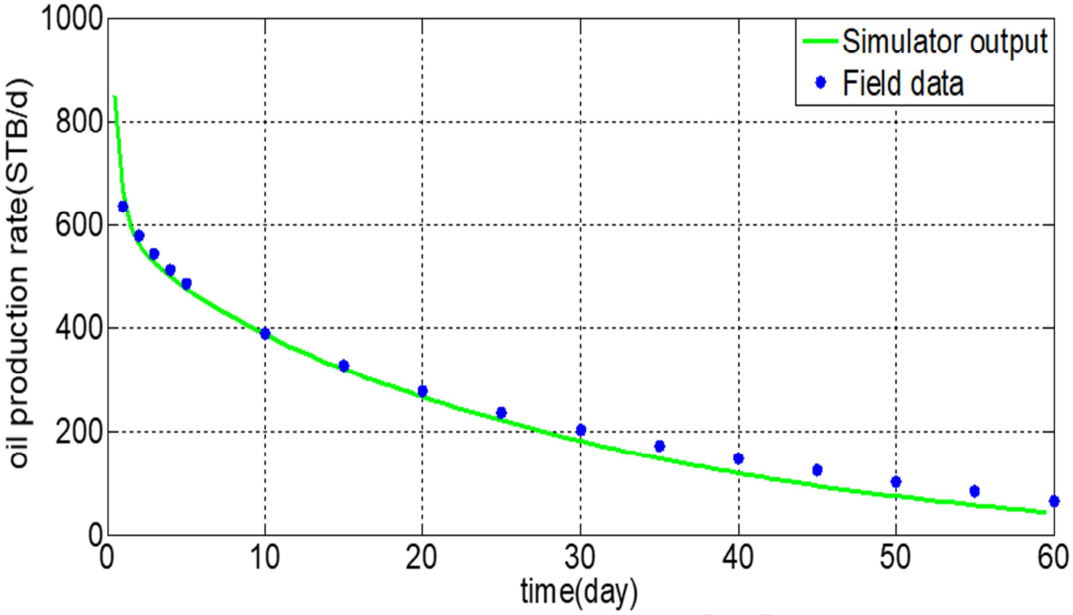

Figure 5: Oil production rate for pressure specified well, (W-2)

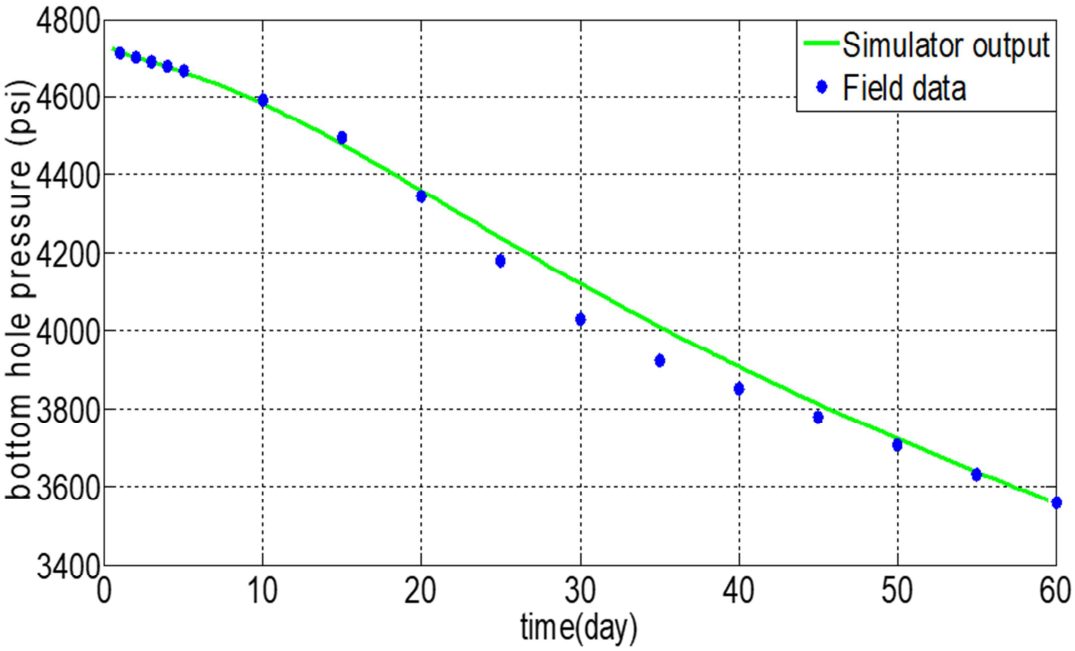

Figure 6: Bottom-hole pressure for gas rate specified well, (W-4)

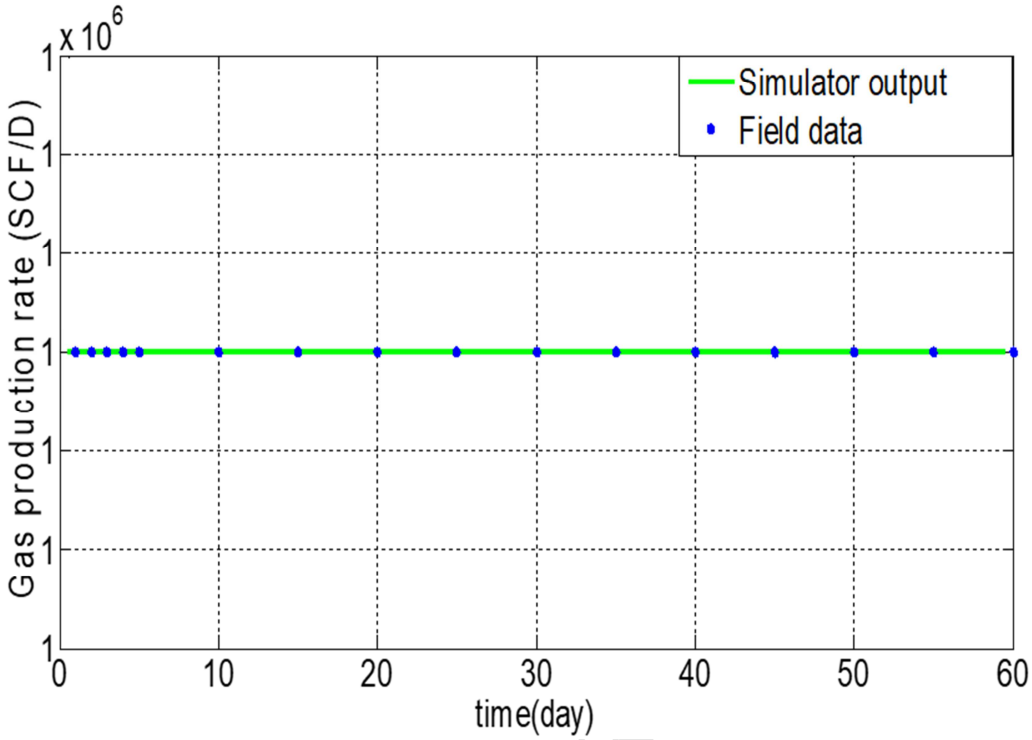

Figure 7: Gas production rate for gas rate specified well, (W-4)

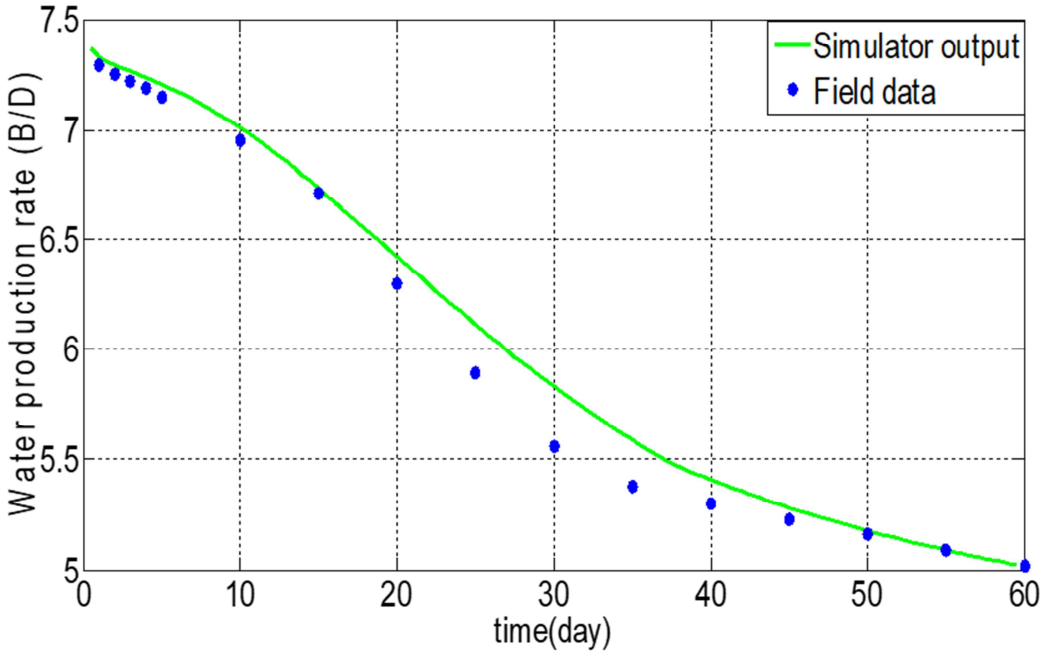

Figure 8: Water production rate for gas rate specified well, (W-4)

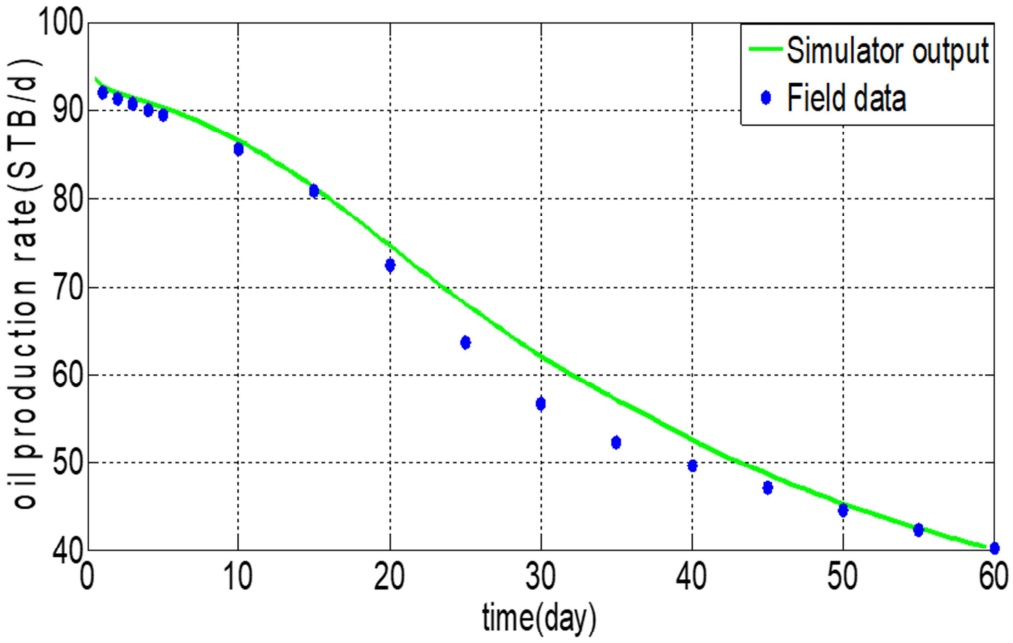

Figure 9: Oil production rate for gas rate specified well, (W-4)

For the second half of this project, reservoir grids were altered to suit what is recommended for fractured grid system using Bennett's algorithm. We assumed a symmetric fracture that extends equal distances on both sides of the wellbore and spans the complete thickness of the formation, as such only 1/4 of the drainage area from the fracture was simulated. Relative permeability and capillary pressure curves for the reservoir are shown in **Figure 10** and **Figure 11**, respectively. Linear relative permeability and zero capillary pressure curves were applied in the fracture. Other reservoir properties are summarized in **Table 1.** The fracture width is increased to maintain numerical stability in the model; however, the porosity and permeability are adjusted accordingly to preserve the conductivity and the material balance (fracture volume).

Table 1: Properties for the model

Parameter	Value
Initial model dimensions (feet)	2000 x 2000
Formation permeability (md)	0.05
Formation porosity (%)	10
Fracture porosity (%)	50

Reservoir pressure (psi)	5830
Reservoir temperature (F)	190
Fracture half length (feet)	210, 410, 700, 1000
Fracture half width (feet)	0.25
Dimensionless fracture conductivity	0.1, 1, 5, 10
Bottom hole pressure (psi)	580
Gas specific gravity	0.6
Initial water saturation	0.5
Leak off volume (bbls)	200
Fluid flow behavior index	0.5, 0.8, 1, 10
Fluid yield stress (Pa)	0-19.49
Fluid consistency index (dyne-$s^{n'}/cm^2$)	40-2000

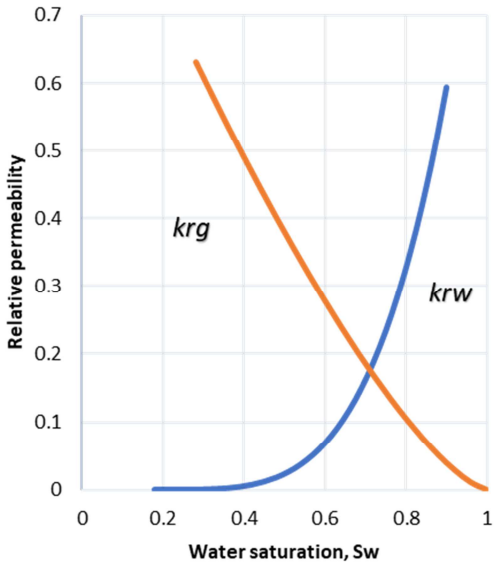

Figure 10: Gas/water relative permeability curve used in the model

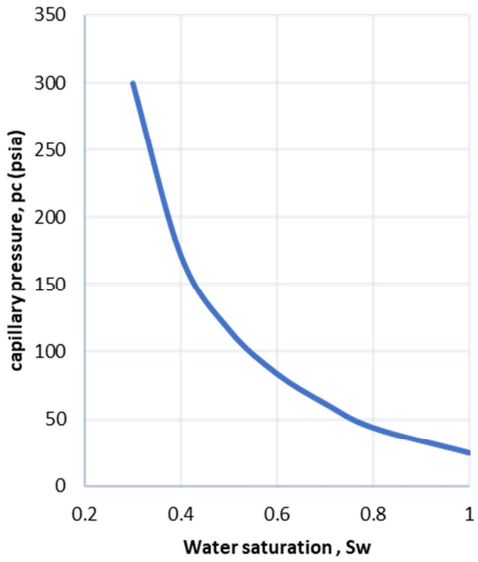

Figure 11: Capillary Pressure curve used in the model

3.2 Initial Conditions

A two-phase fracture propagation model was used to create the formation damage and invaded zone by injecting water for 0.05 and 0.1 of a day under a high pressure of 5830 psi and shutting-in the well for roughly equal amounts of time. 200 barrels of water were injected to create the leak off profile and model formation damage. The leak off fluid was distributed by increasing the fracture conductivity along the specified fracture half-length and time. By specifying the total injection time and the total length of the fracture, the fracture half-length at each time was calculated by the use of Eq. 5 (Friedel, 2006),

$$\frac{x_f(t)}{t^{0.5}} = \frac{x_f}{t_{end}^{0.5}} \qquad Eq.\ 5$$

Pressure and saturation maps at the end of shut-in periods were used to establish the initial conditions for our polymer clean up model, and they are shown in **Figure 13 Figure 12 Figure 14 and Figure 15.** These initial conditions were simulated for all the different scenarios.

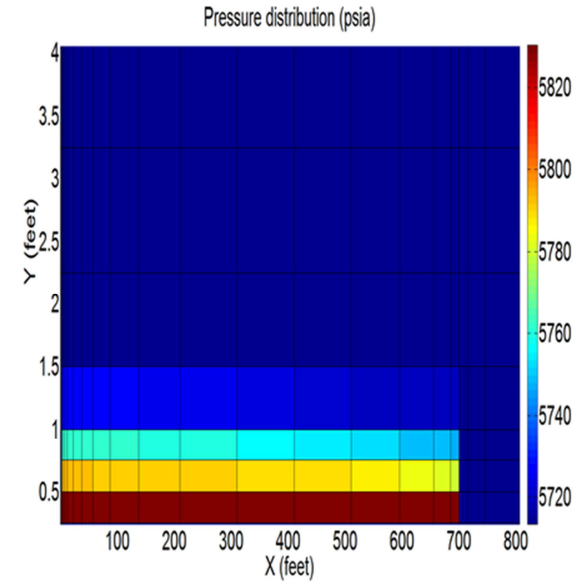

Figure 13: Pressure distribution at the end of first shut-in period for k=0.05md, C_{fd}= 1

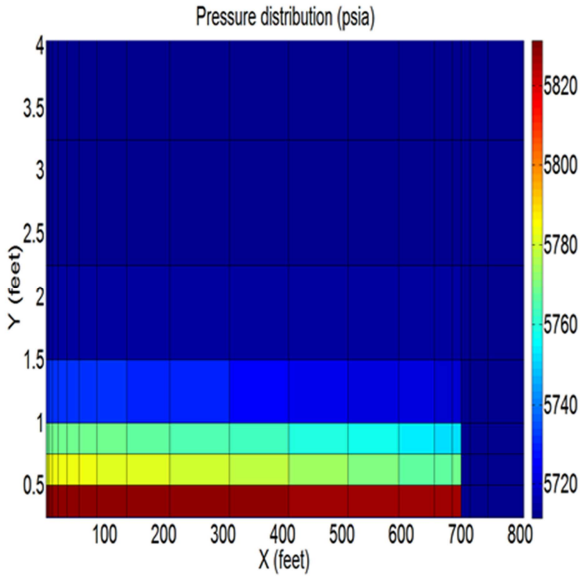

Figure 12: Pressure distribution at the end of first shut-in period for k=0.05md, C_{fd}= 1

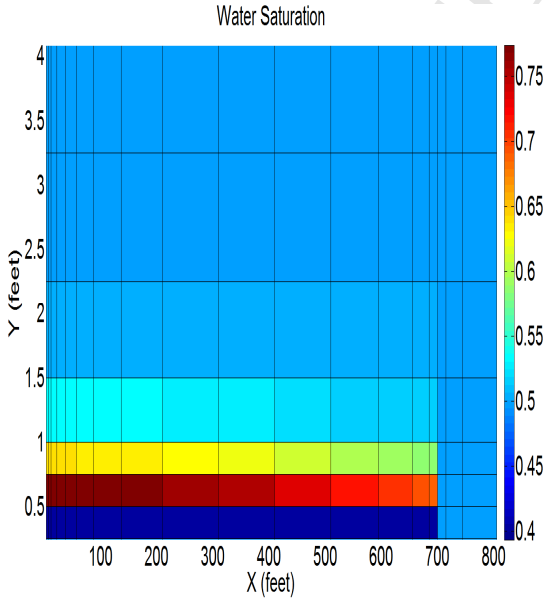

Figure 14: Water Saturation at the end of first Injection period for k=0.05md, C_{fd}= 1

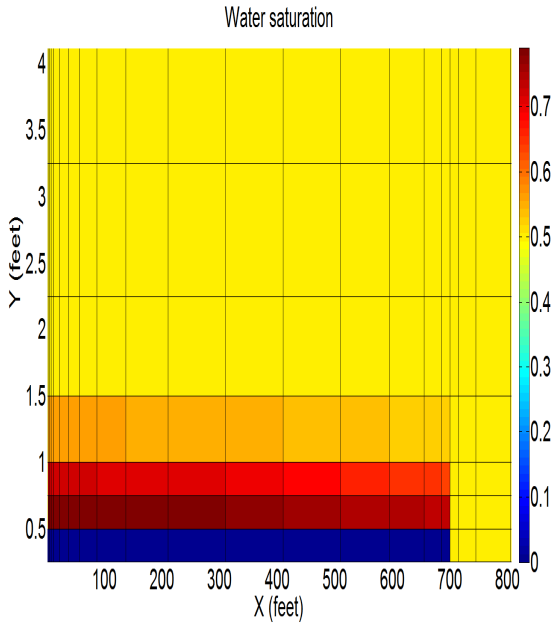

Figure 15: Water Saturation at the end of first shut-in period for k=0.05md, C_{fd}= 1

3.3 Yield Stress Model

Our polymer model was simulated by replacing the water inside the fracture with fracturing fluid (gel) for production simulations. The gel phase was restricted to the fracture. Equations of yield stress and power-law behavior of the gel were used following the work of Yi et al. (Yi, 2004).

$$\tau = \tau_0 + K'(\frac{dv}{dr})^{n'} \qquad Eq.\ 6$$

$$\mu_{eff,nn} = \frac{K'}{12}(9 + \frac{3}{n'})^{n'}(72\ C\ \varphi(S_{nn} - S_{ir,nn})\ k\ k_{r,nn})^{\frac{1-n'}{2}} \qquad Eq.\ 7$$

$$\beta = N_n\sqrt{\frac{\varphi\ C(S_{nn} - S_{ir,nn})}{2kk_{r,nn}}} \qquad Eq.\ 8$$

$$\mu_{nn} = \begin{cases} +\infty & \left(-\frac{\partial\varphi}{\partial L}\right) \le \beta\tau_0 \\ \dfrac{kk_r\left(-\frac{\partial\varphi}{\partial L}\right)}{[\frac{kk_r}{\mu_{eff,nn}}(\left(-\frac{\partial\varphi}{\partial L}\right) - \beta\tau_0)]^{\frac{1}{n'}}} & \left(-\frac{\partial\varphi}{\partial L}\right) > \beta\tau_0 \end{cases} \qquad Eq.\ 9$$

$$N_n = \frac{3n'+1}{2n'+1} - \frac{3(3n'+1)(1-n')}{16(2n'+1)^2(n'+1)} \qquad Eq.\ 10$$

The viscosity value μ_{nn} assigned to a fracture grid is grossly dependent on the potential gradient and the yield point of the gel in that grid. A certain threshold pressure gradient is required to initiate flow. If the potential gradient $\frac{\partial\varphi}{\partial L}$ is greater than the yield stress of the gel, the fracturing fluid will flow to the wellbore. If the potential gradient $\frac{\partial\varphi}{\partial L}$ is less than the yield point of the gel, the fracturing fluid behaves as a solid, and it remains inside the fracture reducing its conductivity. A large viscosity value of $1000000\ cp$ is assigned to the fracturing fluid for our simulation study when the potential gradient is less than the yield stress to simply simulate the lack of movement when pressure gradient is below the defined yield stress.

4 Simulation Results and Analysis

At the end of a fracture treatment process, gel residue resides in and around the fracture obstructing the free flow of hydrocarbons. A fracturing cleanup process is needed to transport these residues from the fracture back to the Earth's surface. Inadequate fracturing fluid cleanup results in a lag in gas breakthrough at the wellbore, gas production is only observed after the first few time steps. The fracture width is slightly increased to 0.5 to maintain numerical stability in the model and the porosity decreased to 0.4 to preserve the material balance. 200 barrels of water were distributed around the fracture to create the initial conditions for all the runs. The total gel volume in the fracture at the end of fluid injection was 638 bbls. The factors under consideration which significantly hamper fluid recovery were investigated for a total simulation time of 100 days and the observed trends are reported as follow.

4.1 Effect of Fracture Conductivity

Dimensionless fracture conductivity provides a mean of optimizing fracture conductivity by varying fracture permeability. Overtime, the conductivity of a fracture can be significantly reduced by proppant crushing, proppant embedment into the formation, increasing stress on proppant, formation damage resulting from gel residue or fluid loss additives, non-Darcy and multiphase flow (Palisch, Duenckel, Bazan, Heidt, & Turk, 2007). The fracture conductivity is defined as the fracture permeability times the fracture propped width as shown in Eq. 11. The higher the fracture conductivity the easier the fluid flows inside the fracture. The dimensionless fracture conductivity, which can be calculated by Eq. 12, accounts for the formation capability of supplying fluid by considering the formation permeability and the fracture half-length.

$$F_D = k_f\, w \qquad \textit{Eq. 11}$$

where F_D is the fracture conductivity, k_f is fracture permeability and w is the fracture propped width

$$C_{fD} = \frac{k_f\, w}{k\, x_f} \qquad \textit{Eq. 12}$$

where C_{fD} is the dimensionless fracture conductivity, k_f is the fracture permeability, w is the fracture propped width, k is the formation permeability and x_f is the fracture half-length

The effect of fracture conductivity for constant rheology of fracturing fluid was investigated by varying the permeability in the fracture while keeping fracture length constant. By increasing the fracture conductivity, the fracture cleans up faster resulting in higher gas production as can be seen in **Figure 16**. Increasing the fracture conductivity from 1 to 10 shows a terrific increase in cumulative gas production relative to an increase in fracture conductivity from 0.1 to 1. However, increasing the dimensionless fracture conductivity for a tight gas reservoir to values higher than 10 would not considerably increase gas flow rates (Wang, Holditch, & McVay, 2010).

4.2 Effect of Fracture Length

In order to enhance the performance of hydraulically fractured wells, accurate estimates of fracture lengths (i.e. created, propped and effective lengths) are important in the choice of fracture design configurations and consequently, a major determinant of the overall success of

the fracture treatment in tight gas reservoirs. The propped length is usually 70% or more of the created length while the effective length is often only 10 to 50% of the propped length (Wang, Holditch, & McVay, 2010). Fracture half lengths estimated from pressure transient test are roughly only 5 to 11% of the designed lengths while fracture lengths determined from reservoir simulation history matching average about 68% of the designed lengths (Lee & Holditch, 1981). The longer the effective fracture length created, the greater the effective stimulation of the well as more of the formation is exposed to the wellbore resulting in higher fluid recovery. Assuming the fracture lengths simulated in this study to be quite representative of the expected effective fracture lengths, it is easy to see that cumulative gas production increases with increasing effective fracture lengths as presented in **Figure 17**.

In designing fracture treatments, it is important to take into account proppant retardation for both water and conventional gel fracturing fluids for a good estimate of the effective fracture lengths (Sharma & Gadde, 2005).

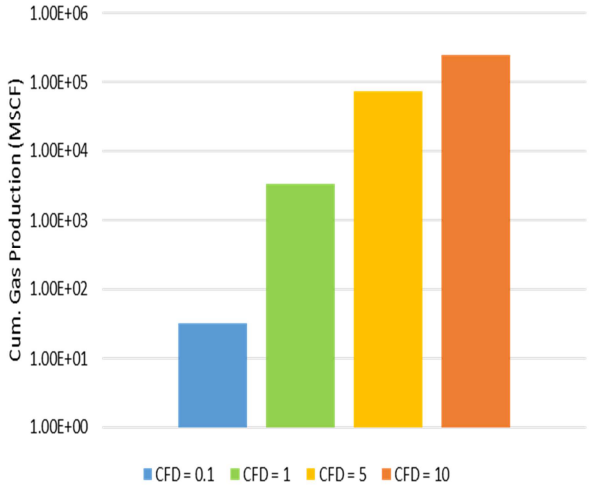

Figure 16: Cumulative gas production at different fracture conductivities, for τ_0=5Pa, n=0.5 and k '=200 dyne-$s^{n\prime}/cm^2$ after 100 days of production

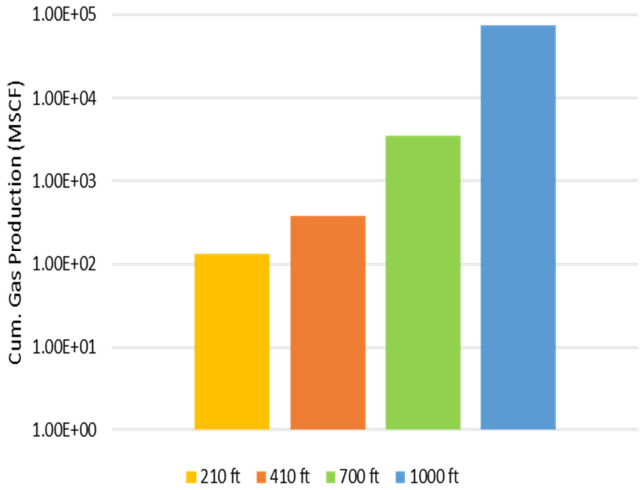

Figure 17: Cumulative gas production for different propped fracture lengths, k= 0.05 md, τ_0=5Pa, n=0.5 and k'=200 dyne-$s^{n\prime}/cm^2$ after 100 days of production

4.3 Effect of Injection Time

Increasing the injection time from 1.2 to 2 hours causes the water saturation around the fracture face to increase by roughly 16%, **Figure 18**. However, with increasing shut-in time from 1.2 to 7.2 hours, the high capillary forces in the formation causes the high water saturation around the fracture face to be further imbibed into the matrix. Thus the immediate water saturation around the fracture face after the second shut-in period is reduced by roughly 7.5 % relative to the first shut-in period, **Figure 19**. This cut in water saturation results in higher gas relative permeability, higher gas saturation around the fracture face and consequently higher gas production for the period under consideration. However, increasing the shut-in time increases the depth of the invaded zone as the water saturation moves further into the formation, **Figure 19**.

The huge pressure buildup around the fracture at the end of injection period is equally dissipated through the formation to near initial conditions at the end of shut-in period, **Figure 21**. Clearly, aqueous phase trapping or water blocking is an important damage mechanism as the high water saturation clogging the pores around the fracture face could severely impede gas flow during recovery.

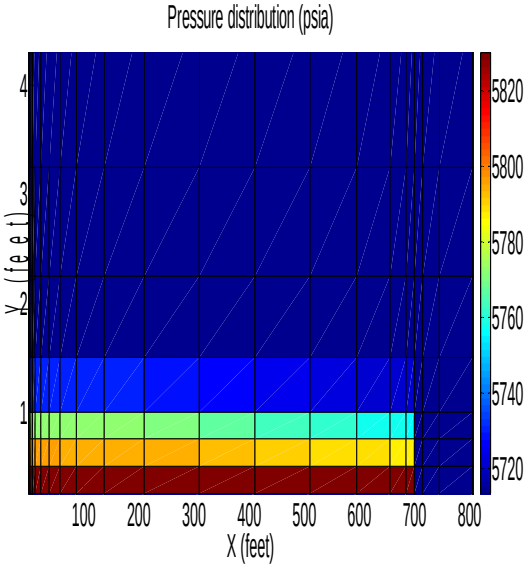
Pressure distribution (psia)
5820
5800
5780
5760
5740
5720
100 200 300 400 500 600 700 800
X (feet)

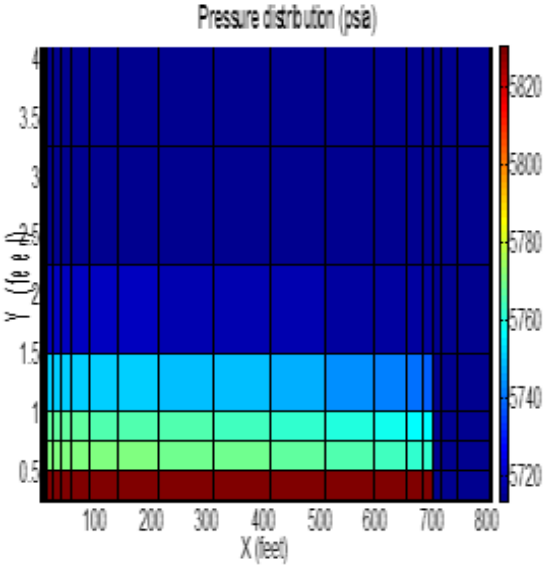
Pressure distribution (psia)
5820
5800
5780
5760
5740
5720
100 200 300 400 500 600 700 800
X (feet)

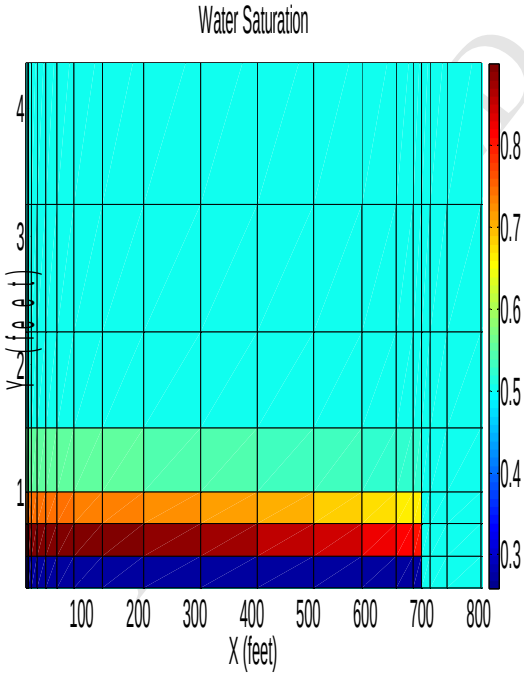
Water Saturation
0.8
0.7
0.6
0.5
0.4
0.3
100 200 300 400 500 600 700 800
X (feet)

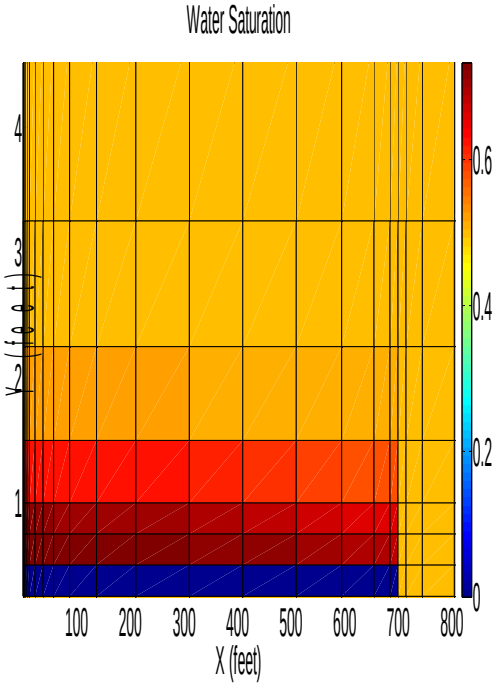
Water Saturation
0.6
0.4
0.2
0
100 200 300 400 500 600 700 800
X (feet)

4.4 Effect of Capillary Pressure

Capillary pressure in the damaged zone increases with increasing levels of damage resulting in lower gas rates and cumulative gas production. Lowering the permeability of the damaged zone equally prevents significant imbibition of water into the undamaged matrix during production, resulting in lower gas relative permeability and consequently lower gas production. From **Figure 22**, it is easy to see that higher values of capillary pressure in the invaded zone can enhance the negative effects of mechanical damage along the fracture face with a yield stress fluid present. The effect of capillary pressure on the fluid recovery was simulated in this study by progressively reducing the capillary forces. Lowering the capillary pressure forces in the formation had quite an effect on fluid recovery, raising the pressure on the lower density fluid (gas) and consequently resulting in higher cumulative gas production. The effect of capillary pressure showed more than a 10% decrease in the gas production as the capillary pressure changed from 10 psi to 300 psi as shown in **Figure 22**.

4.5 Effect of Fluid Type

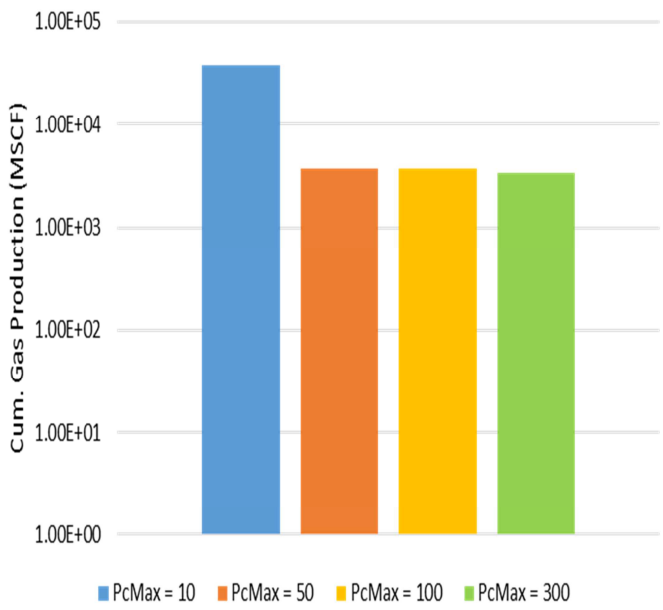

Figure 22: Showing the effect of capillary pressure on cumulative gas production, for C_{fd} =1, k= 0.05 md, τ_0=5Pa, n = 0.5 k'= 200 dyne-$s^{n\prime}/cm^2$ after 100 days of production

The effect of fluid type was simulated by using a shear thinning fluid with yield stress ($\tau_0 = 5, and\ n = 0.5\ or\ 0.8$) , and a Newtonian fluid with ($\tau_0 = 0,\ n = 1$). Cumulative gas production is increased by a factor of 17.16 when the fracturing fluid type was switched from non-Newtonian to Newtonian as can be seen in **Figure 23**; **t**hus, reiterating the importance of ample degradability of fracturing fluids on the fracturing fluid cleanup process.

4.6 Effect of Increasing Breaker Concentration on Yield Stress and Broken Gel Viscosity

Cumulative gas production for an initial guar concentration of 200 $lb/Mgal$ were simulated for the effect of increasing breaker concentration on yield stress of filter cake using the reported correlations in Xu et al. (Xu, Hill, Zhu, & Wang, 2011), and the results are shown in **Figure 24** and **Table 2**.

$$y = -3 * 10^{-5}\, x^3 + 0.0123\, x^2 - 0.9313\, x + 19.828 \qquad \textit{Eq. 13}$$

where y and x are yield stress in Pa and polymer concentration in $lb/Mgal$, respectively. Eq. 13 is valid for polymer concentrations in the range of $0 - 200\ lb/Mgal$.

$$v = -0.0439\, u^3 + 1.3548\, u^2 - 14.6\, u + 62.179 \qquad \textit{Eq. 14}$$

where v and u are polymer concentration in $lb/\ Mgal$ and breaker concentration in $gal/Mgal$, respectively.

Eq. 14 is valid only for a polymer concentration of 200 $lb/Mgal$. Increasing the breaker concentration/enzyme activity reduces the yield stress of gel as per the correlations of Xu et al. resulting in an overall increase in cumulative gas production as presented in **Table 2** (Xu, Hill, Zhu, & Wang, 2011),

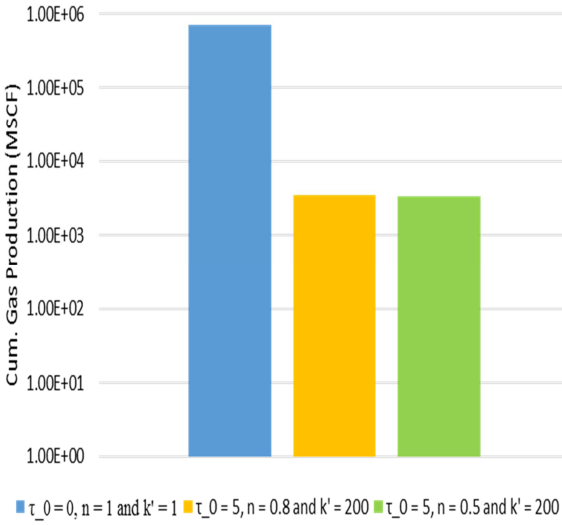

Figure 23: Effect of fluid type on Cumulative Gas production for several values of n and k' after 100 days of production

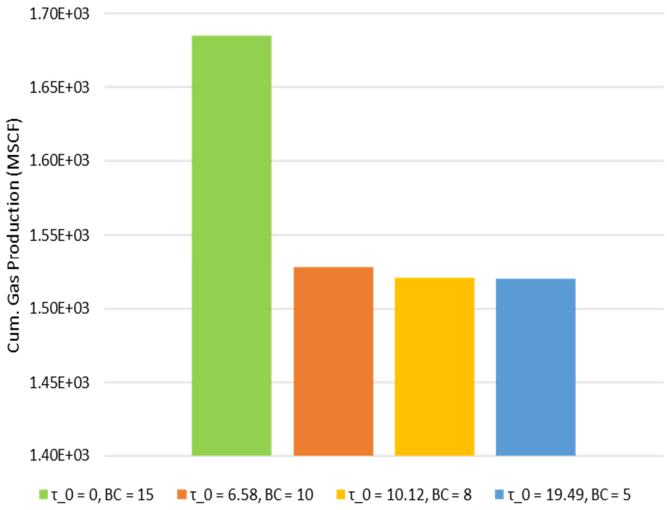

Figure 24: Cumulative gas production showing the effect of increasing breaker concentration (BC) on fracturing fluid yield stress and gel viscosity, for Cf_d = 1 k= 0.05 md after 100 days of production

Table 2: Cumulative fluid production showing the effect of increasing breaker concentration on fracturing fluid yield stress and gel viscosity, for C_fd = 1, k= 0.05 md

Breaker Conc. $(lb/Mgal)$	Fluid yield stress (τ_0/Pa)	Fluid consistency index (k') $(mPa.s^{n'})$	Fluid flow behavior index (n')	Cumulative gas $(MSCF)$
15	0.0	40	0.5	1685
10	6.582	60	0.5	1528
8	10.127	75	0.5	1521
5	19.494	80	0.5	1520

A breaker concentration of 15 $gal/Mgal$ was required to fully degrade yield stress of polymer gel, thus resulting in a near Newtonian fluid. **Figure 24** shows cumulative gas production for increasing values of yield stress and viscosity, respectively. Increasing the yield stress and viscosity of the fracturing fluid adversely affects gas production. For lower values of yield stresses ($\tau_0 = 0.0\ Pa$), the fracture cleans up faster and cumulative gas production is the highest for the lowest value of yield stress ($\tau_0 = 0.0\ Pa$) than for when it is increased to higher values ($\tau_0 = 6.58, 10.13, 19.49\ Pa$) for a total simulation time of 100 days.

4.7 Material Balance Equation for Yield Stress Determination along Fracture Face

For Aqueous fracturing fluids, continuous water imbibition from the fracture face into the formation results in increased polymer concentration on the fracture face (filter cake build up) and consequently higher residual or yield stress values. Assuming an initial Guar concentration of $40lb/Mgal$, the concentration of the polymer gel remaining in the fracture after 1.2 hours of fracturing fluid injection can be calculated from the following material balance equation. This is assuming that the pores are small enough that no polymer invasion occurs into the formation. This assumption is valid for tight and ultra-tight formations.

$$C_{frac} = \frac{C_i V_i}{V_{frac}} \qquad \textit{Eq. 15}$$

where C_i is the initial concentration of polymer injected and C_{frac} is the concentration of polymer gel left behind in the fracture in $lb/Mgal$, V_i, the total volume of injected fluid and V_{frac}, the volume of fluid contained in the fracture pores.

Figure 25 shows how the polymer concentration is changing along the fracture face with distance and time. The polymer concentration decreases as we move further down the fracture and away from the injection well because the fluid volume lost to the formation decreases further down the fracture**.** The guar concentration increases with injection time as the gel residue deposited along the fracture face accumulates over time resulting in higher yield stress values. It is clear from **Figure 25** that the minimum guar concentration, which is the initial guar concentration of 40 lb/Mgal, is at the fracture tip and the maximum guar concentration occurs near the fracture entrance. Eq. 16 and Eq. 17 are expressions which relate the polymer concentration in the fracture with distance down the fracture and injection time, respectively.

$$C_{frac} = -0.000008\,x^2 + 0.0002x + 49.765 \qquad \textit{Eq. 16}$$

$$C_{frac} = -1.4212\,t^2 + 9.85t + 40 \qquad \textit{Eq. 17}$$

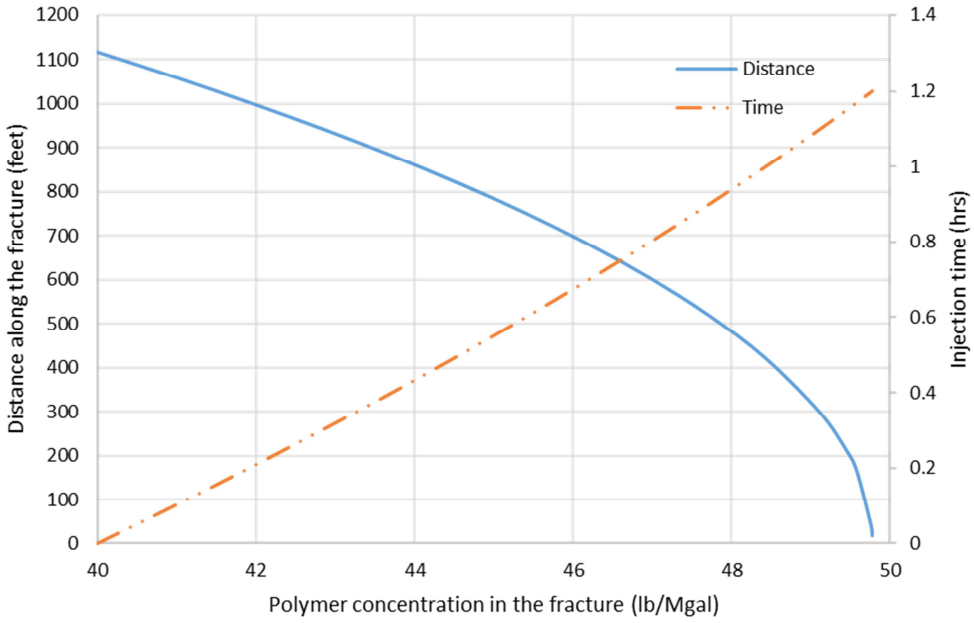

Figure 25: Distance along the fracture and injection time versus the polymer concentration in the fracture

Yield stress values along the fracture face are calculated from polymer concentration according to Xu et al. (Xu, Hill, Zhu, & Wang, 2011) correlation. The yield stress along the fracture face is found to increase with increasing fluid loss to the formation as shown in **Figure 26**. The rate at which the yield stress (τ) is increasing or the filter cake is building up is proportional to the square of the volume of fluid lost (PVs) to the formation as given by the following expression, Eq. 18.

$$\tau = 3.4146\, PVs^2 - 14.97 PVs + 16.511 \qquad Eq.\ 18$$

Pressure distribution along the fracture face for an initial guar concentration of 40 $lb/Mgal$ shows a sharp decline in pressure a few feet away from the producing well and decreases

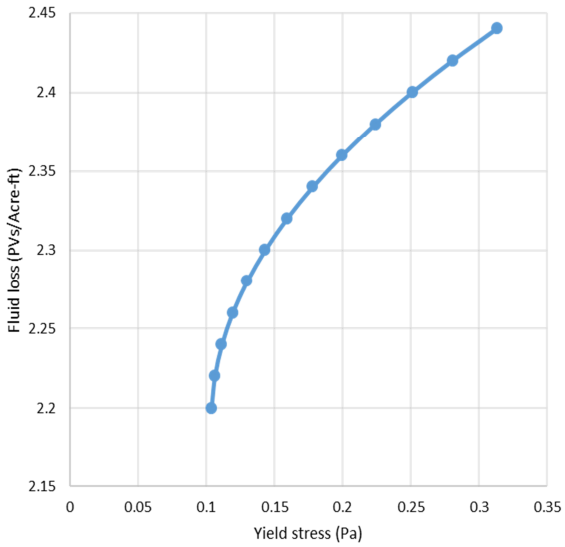

Figure 26: Yield stress increasing as more fluid is being lost along the fracture face for an initial guar concentration of 40 $lb/Mgal$

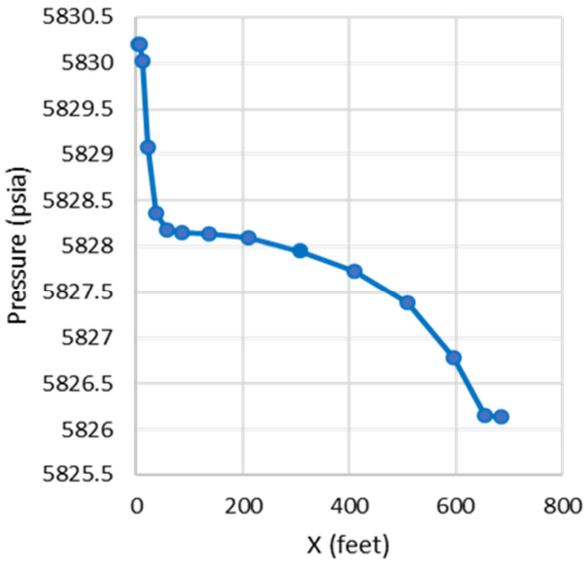

Figure 27: Pressure distribution along the fracture face for an initial guar concentration of 40 $lb/Mgal$

even further as we move further down the fracture face, **Figure 27**.

Several values of initial guar concentration were tested, yield stress variation with fluid loss volume, **Figure 28**, and polymer concentration, **Figure 29**, along the fracture face were calculated. The variation in yield stress distribution along the fracture face becomes more significant with increasing polymer concentration. The relationship between polymer concentration variations with yield stress along the fracture face becomes more linear for increasing values of initial guar concentration. In addition, there exist a critical breaker concentration value for which the yield stress of the fracturing fluid generated along the fracture face is reduced to zero. This cut-off breaker concentration increases linearly with guar concentration, **Figure 30**. This is in conformity with the results reported in Xu et al. (Xu, Hill, Zhu, & Wang, 2011). Cumulative gas production for each of these scenarios were simulated and reported in **Figure 31**. A more effective breaker results in lower viscosity and yield stress of filter cake in the fracture, which results in a more efficient cleanup of the fracture and a larger effective fracture length available for production.

Guar gum is proven to generate the most favorable results when it comes to crosslinking, generating viscoelastic fluids, and carrying proppants. Gar-based fluids have also shown fast degradation when appropriate concentrations of breaker was added to the solution. This model

helps designing a fracturing fluid with favorable cleanup properties that causes minimum amounts of damage to the proppant pack.

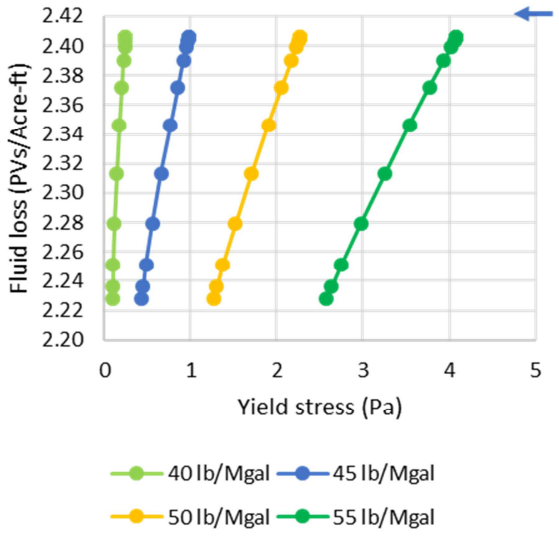

Figure 28: Cumulative gas production at different initial guar concentrations resulting in varying yield stress along the fracture face

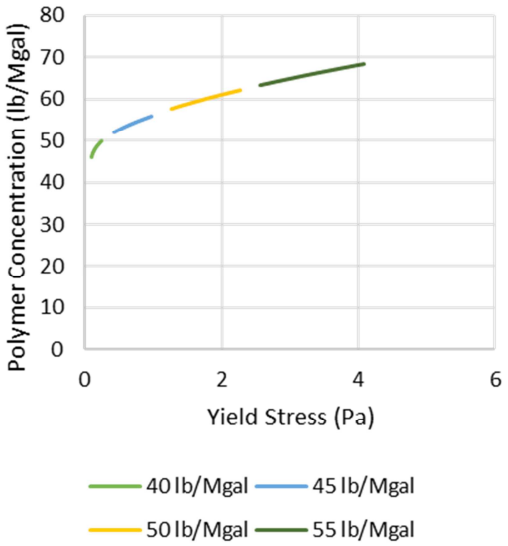

Figure 29: Yield stress variation with fluid loss volume along the fracture face for different guar concentrations

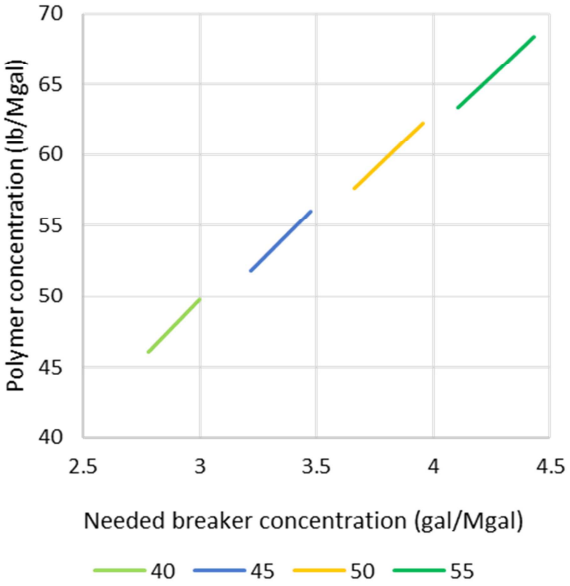

Figure 30: Polymer concentration versus yield stress generated along the fracture face for different initial guar concentrations

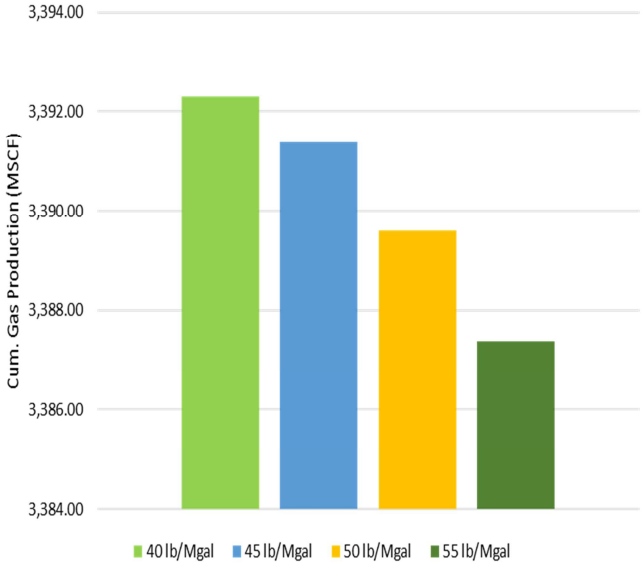

Figure 31: Polymer concentration versus needed breaker concentration to curb yield stress along the fracture face after 100 days of production

5 Conclusions

1. The three-phase IMPES simulator developed for this study is stable, fast and robust. It accurately models three-phase flow through any structured grid.
2. A shift in the capillary pressure curve to higher values significantly reduces fluid recovery. Increasing the capillary pressure to a maximum of 350.10 psi resulted in a 10.4% decrease in cumulative gas production.
3. For tight gas formations ($k = 0.05\ md$), fluid recovery increases with increasing shut-in time, increasing fracture conductivity and fracture length irrespective of the yield stress of the fracturing fluid.
4. Increasing the breaker concentration for a more complete degradation of the yield stress of the fracturing fluid would significantly enhance production.
5. The rate of increase in the yield stress of the fracturing fluid along the fracture face is proportional to the square of the volume of fluid loss (PVs) to the formation.
6. For low permeability reservoirs, mechanically induced formation damage combined with hydraulic damage tends to be the most significant.
7. Lastly, it is more realistic to simulate yield stress variation along the fracture face rather than assuming constant values because the fluid loss to the formation and the polymer concentration distribution along the fracture face decreases as we move away from the injection well.

6 Acknowledgment

The authors would like to thank the Kansas Interdisciplinary Consortium Carbonates (KICC) for partially funding this project. We would like to acknowledge the School of Engineering at the University of Kansas for partially funding this project using the Graduate Research Funds. Our appreciation is extended to MATLAB for providing an educational license to the University of Kansas.

Nomenclature

$\frac{dv}{dr} =$ shear rate (s^{-1})
$\tau_o =$ yield stress (Pa)
$\frac{\partial \varphi}{\partial L} =$ potential gradients
$\varphi =$ rock porosity (fraction)
$k_{rw} =$ relative permeability to water, md
$k_d =$ permeability of damaged zone, md
$k_{rg} =$ relative permeability to gas, md
$PVs =$ fluid volume in pore volume units /Acres $-$ ft
$k' =$ consistency index, non $-$ Newtonian fluid (kPa • sn')
$C_{fd} =$ dimensionless fracture conductivity
$n =$ behavior index, non $-$ Newtonian fluid
$k =$ formation permeability, md
$\mu =$ viscosity of fluid (cp)
$P_c =$ capillary pressure (psi)
$x_f =$ fracture half $-$ length (ft)

μ_{nn} = viscosity of gel (cp)
BC = breaker concentraton (lb/Mgal)
S_w = water saturation (fraction)

References

Agarwal, R., Carter, R., & Pollock, C. (1979). Evaluation and Performance Prediction of Low-Permeability Gas Wells Stimulated by Massive Hydraulic Fracturing. SPE paper 6838. *Journal of Petroleum Technology*. doi:10.2118/6838-PA

Al-Fariss, T., & Pinder, K. (1984). Flow through Porous Media of a Shear-thinning Liquid with Yield Stress. SPE paper 13840. Society of Petroleum Engineers. doi:SPE-13840-MS

Al-Rbeawi, S. (2016, September). New technique for determining rate dependent skin factor & non-Darcy coefficient. *Journal of Natural Gas Science and Engineering, 35 Part A*, 1044-1058.

Al-Rbeawi, S. (2018, November). Performance-Based Comparison for Hydraulically Fractured Tight and Shale-Gas Reservoirs With and Without Non-Darcy-Flow Effect. SPE paper 194011. *SPE Reservoir Evaluation and Engineering, 21*(04).

Ayoub, J. A., Hutchins, R. D., van der Bas, F., Cobianco, S., Emiliani, C. N., Glover, M. D., . . . Turk, G. A. (2006). New Findings in Fracture Clean-up Change Common Industry Perceptions. SPE paper 98746. *SPE International Symposium and Exhibition on Formation Damage Control*. Lafayette: Society of Petroleum Engineers. doi:10.2118/98746-MS

Barati, R., Hutchins, R., Friedel, T., Ayoub, J., Dessinges, M.-N., & England, K. (2009). Fracture Impact of Yield Stress and Fracture-Face Damage on Production With a Three-Phase 2D Model. SPE paper 111457. *SPE Production & Operations*. doi:10.2118/111457-PA

Bennett, C., Reynolds, A., Raghavan, R., & Elbel, J. (1986). Performance of Finite-Conductivity, Vertically Fractured Wells in Single-Layer Reservoirs. SPE paper 11029 . *SPE Formation Evaluation*. doi:10.2118/11029-PA

Davies, D. R., & Kuiper, T. (1988). Fracture Conductivity in Hydraulic Fracture Stimulation. SPE paper 17655. *Journal of Petroleum Technology*. doi:10.2118/17655-PA

Economides, M. J., & Nolte, K. G. (2000). *Reservoir Stimulation* (Third ed.). John Wiley & Sons Ltd. doi:ISBN-10: 0471491926

Ertekin, T., Abou-kassem, J., & King, G. (2001). *Basic Applied Reservoir Simulation*. Richardson: Society of Petroleum Engineers. doi:ISBN: 978-1-55563-089-8

Færgestad, I. (2016). *The Defining Series: Formation Damage.* Schlumberger. Retrieved from http://www.slb.com/-/media/Files/resources/oilfield_review/defining_series/Defining-Formation-Damage.pdf

Friedel, T. (2006). Numerical Investigation on Hydraulic Fracture Cleanup and its Impact on the Productivity of a Gas Well with a non-Newtonian Fluid Model. SPE paper 99445. *SPE Gas Technology Symposium.* Calgary: Society of Petroleum Engineers. doi:10.2118/99445-MS

Gdanski, R., Fulton, D., & Shen, C. (2006). Fracture Face Skin Evolution During Cleanup. SPE paper 101083. *SPE Annual Technical Conference and Exhibition.* San Antonio: Society of Petroleum Engineers. doi:10.2118/101083-MS

Gdanski, R., Fulton, D., & Shen, C. (2009). Fracture-Face-Skin Evolution During Cleanup. SPE paper 101083. *SPE Production & Operations*. doi:10.2118/101083-PA

Gdanski, R., Weaver, J., Slabaugh, B., Walters, H., & Parker, M. (2005). Fracture Face Damage – It Matters. SPE paper 94649. *SPE European Formation Damage Conference.* Sheveningen: Society of Petroleum Engineers. doi:10.2118/94649-MS

Holditch, S. A. (1979). Factors Affecting Water Blocking and Gas Flow From Hydraulically Fractured Gas Wells. SPE paper 7561. *Journal of Petroleum Technology*. doi:10.2118/7561-PA

Holditch, S. A., & Tschirhart, N. (2005). Optimal Stimulation Treatments in Tight Gas Sands. SPE paper 96104. *SPE Annual Technical Conference and Exhibition.* Dallas: Society of Petroleum Engineers. doi:10.2118/96104-MS

Lee, W., & Holditch, S. (1981). Fracture Evaluation With Pressure Transient Testing in Low-Permeability Gas Reservoirs. SPE paper 9975. *Journal of Petroleum Technology*. doi:10.2118/9975-PA

May, E. A., Britt, L. K., & Nolte, K. G. (1997). The Effect of Yield Stress on Fracture Fluid Cleanup. SPE paper 38619. *SPE Annual Technical Conference and Exhibition.* San Antonio: Society of Petroleum Engineers. doi:10.2118/38619-MS

Odumabo, S., Karpyn, Z., & Ayala, L. (2014). Investigation of gas flow hindrance due to fracturing fluid leakoff in low permeability sandstones. *Journal of Natural Gas Science and Engineering, 17*, 1-12. doi:https://doi.org/10.1016/j.jngse.2013.12.002

Palisch, T., Duenckel, R., Bazan, L., Heidt, J., & Turk, G. (2007, January 1). Determining Realistic Fracture Conductivity and Understanding its Impact on Well Performance - Theory and Field Examples. SPE paper 106301. *SPE Hydraulic Fracturing Technology Conference.* College Station: Society of Petroleum Engineers. doi:10.2118/106301-MS

Qutob, H., & Byrne, M. (2015). Formation Damage in Tight Gas Reservoirs. SPE paper 174237. *SPE European Formation Damage Conference and Exhibition.* Budapest: Society of Petroleum Engineers. doi:10.2118/174237-MS

Seright, R. S. (2004). *Conformance Improvement Using Gels.* Socorro: Annual Technical Progress Report No. DOE/BS/15316-6, Contract No. DE-FC26-01BC15316.

Sharma, M., & Gadde, P. (2005). The Impact of Proppant Retardation on Propped Fracture Lengths. SPE paper 97106. *SPE Annual Technical Conference and Exhibition.* Dallas: Society of Petroleum Engineers. doi:10.2118/97106-MS

Voneiff, G., Robinson, B., & Holditch, S. (1996). The Effects of Unbroken Fracture Fluid on Gas Well Performance. SPE paper 26664. *SPE Production & Facilities*. doi:10.2118/26664-PA

Wang, J. Y., Holditch, S., & McVay, D. (2010). Modeling Fracture-Fluid Cleanup in Tight-Gas Wells. SPE paper 119624. *SPE Journal*. doi:10.2118/119624-PA

Wang, J., Holditch, S., & McVay, D. (2012). Effect of gel damage on fracture fluid cleanup and long-term recovery in tight gas reservoirs. *Journal of Natural Gas Science and Engineering, 9*, 108-118. doi:https://doi.org/10.1016/j.jngse.2012.05.007

Xu, B., Hill, A., Zhu, D., & Wang, L. (2011). Experimental Evaluation of Guar-Fracture-Fluid Filter-Cake Behavior. SPE paper 140686. *SPE Production & Operations*. doi:10.2118/140686-PA

Yi, X. (2004). Model for Displacement of Herschel-Bulkley Non-Newtonian Fluid by Newtonian Fluid in Porous Media and Its Application in Fracturing Fluid Cleanup. SPE paper 86491. *SPE International Symposium and Exhibition on Formation Damage Control.* Lafayette: Society of Petroleum Engineers. doi:10.2118/86491-MS

Zoveidavianpoor, M., & Gharibi, A. (2015). Application of polymers for coating of proppant in hydraulic fracturing of subterraneous formations: A comprehensive review. *Journal of Natural Gas Science and Engineering, 24*, 197-209. doi:https://doi.org/10.1016/j.jngse.2015.03.024

- A three-phase simulator was developed to simulate the hydraulic fracture cleanup
- Fluid recovery increases with shut-in time, conductivity and fracture length
- Yield stress increase is proportional to the square of the fluid loss volume
- Mechanically-induced damage with hydraulic damage is the most significant
- Simulation of yield stress variation along the fracture is crucial to production